

# Extending the Application of the Constrained Interpolation Profile (CIP) Scheme from Single-Phase to Two-Phase Hydrothermal Reservoir Simulations

Mitsuo Matsumoto

Exploration & Production Department, Idemitsu Kosan Co., Ltd., 3-1-1 Marunouchi, Chiyoda-ku, Tokyo 100-8321, Japan

mitsuo.matsumoto@idemitsu.com

**Keywords:** Numerical reservoir simulation, CIP scheme, Advection, Numerical dispersion

## ABSTRACT

The application of the Constrained Interpolation Profile (CIP) scheme is extended from single-phase to two-phase one-dimensional hydrothermal reservoir simulations. This extension not only applies the CIP scheme to the advection term of a conservation equation for each phase as in single-phase problems but also evaluates its applicability using a dimensionless parameter called ‘applicability index.’ The applicability index indicates the relative absolute difference between the advancing velocities of the distribution of specific enthalpy due to flow and phase transition front. If the applicability index is exactly or nearly zero, the CIP scheme is applicable because the difference is insignificant. On the other hand, if the value of the applicability index becomes greater than zero, the CIP scheme is inapplicable because the difference becomes significant. The application of the CIP scheme in the inapplicable condition results in numerical failures, such as the degradation of convergence in Newton-Raphson iteration and oscillating distribution of liquid saturation. The conventional first-order upstream difference scheme is adopted when the CIP scheme is inapplicable.

Two contrasting examples demonstrate the applicability of the CIP scheme. The first example injects hot fluid into the initially single-phase reservoir with relatively low permeability. The second example injects cold water into the initially two-phase reservoir with relatively high permeability. In the former example, the CIP scheme is inapplicable in the entire two-phase region expanding from the source. On the other hand, in the latter example, the CIP scheme is applicable in the phase transition zone where liquid saturation is changing with the sweeping of the single-phase region expanding from the source. The numerical failures were overcome as demonstrated in the comparison with a trial run adopting the CIP scheme regardless of the applicability index.

## 1. INTRODUCTION

The reliability of the simulated advection of heat and chemical components in hydrothermal reservoirs is one of the key technical issues in estimating both the productivity of reservoirs and impacts of production and/or re-injection in the environment. Reliable simulation models enable the accurate prediction of reservoir productivity and environmental impacts based on good interpretations of observations, such as temporal changes in temperature and tracer concentration in the produced fluid. The reliable simulation models require not only observed data with enough quantity and quality but also enough numerical accuracy in solving governing equations numerically. To improve the numerical accuracy, the author has proposed the application of the Constrained Interpolation Profile (CIP) scheme to single-phase reservoir simulations (Matsumoto, 2012; Matsumoto 2015).

CIP is a robust scheme with high-order accuracy and is applicable to a wide range of problems governed by hyperbolic-type equations (Yabe and Aoki, 1991; Yabe et al., 1991). The theoretical background of this scheme is a simple concept of interpolating a function distribution among discretized grid points using a cubic polynomial that is determined by the values of the function and its partial derivatives at each grid point. These partial derivatives are defined as independent variables and constrained by equations derived by partially differentiating the original governing equation. The author proved that the CIP scheme yields considerable differences from the numerical solutions obtained by adopting the conventional first-order upstream difference scheme in the problems characterized by predominant advection (Matsumoto, 2015).

In this workshop, the author demonstrates an extension of the abovementioned reservoir simulations adopting the CIP scheme to two-phase one-dimensional problems. As a result of trial and error in investigating various schemes for this extension, the author has found that the application of the CIP scheme to two-phase problems is only valid under a limited condition. This valid condition has been derived based on a schematic consideration and verified by numerical experiments. Two examples demonstrate successful simulations determining whether the CIP scheme is applicable and adopting it in the valid condition. A trial run also demonstrates that applying the CIP scheme regardless of the condition results in numerical failures, such as the degradation of convergence in Newton-Raphson iteration and oscillating distribution of liquid saturation. In addition to the extension to two-phase problems, the advancing scheme of the non-advection terms is also modified from semi-implicit to fully implicit scheme to improve numerical stability.

## 2. MATHEMATICAL MODEL

Let us consider a mathematical model representing a two-phase flow of water and steam in a one-dimensional Cartesian coordinate system. Our mathematical model is essentially identical to the model adopted in the multi-purpose reservoir simulator HYDROTHERM (Kipp et al., 2008). In this study, we assume that the physical properties of rocks are uniform. Re-arranging this mathematical model, we obtain the following expressions of mass and enthalpy conservations:

$$\partial_t M_l + \partial_t M_g = -U_l \partial_x M_l - U_g \partial_x M_g - M_l \partial_x U_l - M_g \partial_x U_g + q_M, \quad (1)$$

$$\partial_t H_l + \partial_t H_g + \partial_t H_m = -U_l \partial_x H_l - U_g \partial_x H_g - H_l \partial_x U_l - H_g \partial_x U_g + \lambda \partial_{xx} T + q_H. \quad (2)$$

The symbols are defined in the nomenclature at the end of this paper. The nomenclature also describes the mathematical definitions of some symbols. The details of our mathematical model can be reviewed by referring to these definitions. To apply the CIP scheme, we also consider the equations derived by differentiating Eqs. (1) and (2) as follows:

$$\partial_t M_{lx} + \partial_t M_{gx} = -U_l \partial_x M_{lx} - U_g \partial_x M_{gx} - M_{lx} \partial_x U_l - M_{gx} \partial_x U_g + \partial_x \theta_M, \quad (3)$$

$$\partial_t H_{lx} + \partial_t H_{gx} + \partial_t H_{mx} = -U_l \partial_x H_{lx} - U_g \partial_x H_{gx} - H_{lx} \partial_x U_l - H_{gx} \partial_x U_g + \partial_x \theta_H, \quad (4)$$

where

$$\theta_M = -M_l \partial_x U_l - M_g \partial_x U_g + q_M, \quad (5)$$

$$\theta_H = -H_l \partial_x U_l - H_g \partial_x U_g + \lambda \partial_{xx} T + q_H. \quad (6)$$

Note that the symbol  $\partial$  denotes a partial derivative with respect to its subscript, whose number indicates the order of partial derivative (e.g.,  $\partial_{xx} = \partial^2 / \partial x^2$ ). These partial derivatives are approximated numerically, whereas each symbol with the subscript  $x$  (e.g.,  $M_{lx}$ ) denotes a gradient that has a value as an independent variable. Each right-hand side of Eqs. (1)-(4) intends to separate the advection terms (first and second terms) and non-advection terms to adopt the time-splitting method and solve the advection and non-advection terms in separate procedures by selecting the appropriate numerical schemes for each procedure.

### 3. NUMERICAL TECHNIQUES

#### 3.1 Separately solving the advection and non-advection terms

Adopting the time-splitting method, we advance Eqs. (1)-(4) through two procedures for advancing the advection and non-advection terms separately. The first procedure separately solves each advection term of Eqs. (1)-(4) written as follows:

$$\partial_t \Phi_p = -U_p \partial_x \Phi_p, \quad (7)$$

$$\partial_t \Phi_{px} = -U_p \partial_x \Phi_{px}, \quad (8)$$

where the symbol  $\Phi$  and subscript  $p$  are substituted by the symbol  $M$  or  $H$  and subscript  $l$  or  $g$ , respectively. As a result, we obtain four pairs of the advection equation. Applying the CIP scheme to advance each pair of the advection equation as described by Yabe and Aoki (1991), we obtain the values of  $M_l$ ,  $M_g$ ,  $H_l$ ,  $H_g$ , and their gradients at the auxiliary time step that is defined by adopting the time-splitting method. During this first procedure, we assume that the enthalpy contained in the rock matrix  $H_m$  and its gradient  $H_{mx}$  is constant. If the CIP scheme is inapplicable as mentioned below, the conventional first-order upstream difference scheme is adopted temporarily to improve the robustness of the numerical computation. The author does not agree that the first-order upstream difference scheme is always the best choice in the inapplicable regime of the CIP scheme. Future study will establish the numerical technique completely covering both the applicable and inapplicable regimes of the CIP scheme.

Based on the result of the first procedure, the second procedure advances the non-advection terms written as follows:

$$\partial_t (M_l + M_g) = -M_l \partial_x U_l - M_g \partial_x U_g + q_M, \quad (9)$$

$$\partial_t (H_l + H_g + H_m) = -H_l \partial_x U_l - H_g \partial_x U_g + \lambda \partial_{xx} T + q_H, \quad (10)$$

$$\partial_t (M_{lx} + M_{gx}) = -M_{lx} \partial_x U_l - M_{gx} \partial_x U_g + \partial_x \theta_M, \quad (11)$$

$$\partial_t (H_{lx} + H_{gx} + H_{mx}) = -H_{lx} \partial_x U_l - H_{gx} \partial_x U_g + \partial_x \theta_H. \quad (12)$$

To solve the non-advection terms numerically, we adopt the conventional finite difference scheme. Discretizing Eqs. (9) and (10) and the equations describing the boundary conditions, we obtain and solve the system of non-linear equations with respect to pressure  $P$  and mean specific enthalpy of water and steam  $h$  at each grid point. Hereafter, we define  $h$  as ‘specific enthalpy.’ The

Newton-Raphson method is adopted to solve this system numerically. Based on the determined pressure and specific enthalpy at each grid point, the discretized expressions of Eqs. (11) and (12) and the boundary conditions form a non-linear system with respect to the gradients of pressure  $P_x$  and specific enthalpy  $h_x$  at each grid point. This system is again solved numerically by the Newton-Raphson method. Thus, all variables at the next time step can be computed as the functions of pressure, specific enthalpy, and their gradients. Note that the flow velocity  $U_p$  appearing in Eqs. (7) and (8) are computed implicitly. Thus, the computation of the first procedure to solve the advection terms is involved in every iterative procedure of the Newton-Raphson method.

The thermodynamic functions with respect to pressure and specific enthalpy are computed using the equation of state for water and steam IAPWS-IF97 (IAPWS, 2001; IAPWS, 2004a; IAPWS, 2004b; IAPWS, 2005; IAPWS, 2007) developed by the International Association for the Properties of Water and Steam (IAPWS). The viscosity of water and steam involved in the definitions of the flow velocities are also computed using the empirical equation developed by IAPWS (IAPWS, 1997). The linear system in every iterative procedure of the Newton-Raphson method is solved directly using the multipurpose library of linear algebra LAPACK (Anderson et al., 1999). The Jacobian that also appeared in the Newton-Raphson method is approximated using finite differences.

### 3.2 Applicability of the CIP scheme

Applying the abovementioned numerical technique in adopting only the CIP scheme regardless of the condition, the author often experienced numerical failures, such as the degradation of convergence in the Newton-Raphson iteration and oscillating distribution of liquid saturation. The author concludes that the applicability of the CIP scheme is limited based on a schematic consideration in terms of the difference between the advancing velocities of the distribution of specific enthalpy due to flow and phase transition front. Figure 1 shows an example of this consideration schematically. Let us consider the distribution of specific enthalpy  $h$  advancing from an upstream to the downstream region with velocity  $u$  as a result of the flow of water and/or steam. Note that the shape of this distribution is assumed to be maintained during the flow for simplicity. Particularly, the change in this distribution can be approximated to translation. Assuming an approximately steady-state pressure distribution, the constant distribution of the specific enthalpy of saturated water  $h'$  can be superimposed on the advancing distribution of specific enthalpy  $h$ . The intersection of these two distributions corresponds to the boiling front advancing with velocity  $u'$ .

The advancing velocity of the boiling front  $u'$  is different from that of the distribution of specific enthalpy  $u$  unless the distribution of the specific enthalpy of saturated water  $h'$  is approximately uniform or the distribution of specific enthalpy  $h$  has an extremely high gradient. Assuming linear distributions for simplicity as shown in Figure 1, we obtain the following relationship using simple geometrics:

$$\left| \frac{u - u'}{u} \right| = \left| \frac{d_p h'}{\partial_x P / \partial_x h} \right|, \quad (13)$$

where we regard the specific enthalpy of saturated water  $h'$  as a function of pressure and apply the chain rule. Similarly, we can derive the same expression with respect to the specific enthalpy of saturated steam. Further generalization yields the following expression:

$$\left| \frac{u - u'}{u} \right| = \left| \left( \frac{\partial_p h}{\partial_x P} \right)_S \frac{\partial_x P}{\partial_x h} \right|, \quad (14)$$

where the ordinary derivative in Eq. (13) is substituted by the partial derivative of specific enthalpy  $(\partial_p h)_S$  that is regarded as a function of pressure  $P$  and liquid saturation  $S$ . Hereafter, we define the dimensionless parameter defined by Eq. (14) as ‘applicability index’ denoted by the symbol  $A$ .

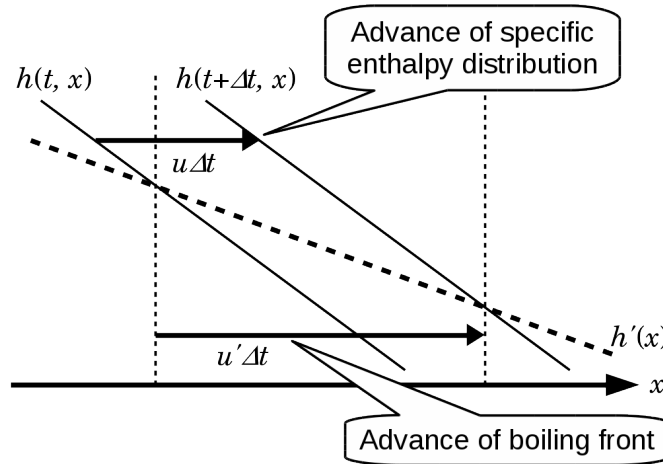


**Figure 1: Schematic diagram describing the difference between the advancing velocities of the distribution of specific enthalpy due to flow and boiling front.**

The applicability index estimates the relative difference between the advancing velocities of the distribution of specific enthalpy due to flow and phase transition front with an arbitrary value of liquid saturation. In the regime of  $A \approx 0$ , the phase transition is controlled by advection predominantly, which may result in the distributions of mass and enthalpy for each phase ( $M_l, M_g, H_l, H_g$ ) advancing with a flow velocity with maintained shapes. We can accurately simulate these advancing distributions adopting the CIP scheme. For physical aspects, the applicability index tends to be nearly zero in problems of flows with a high-contrast temperature distribution in high-permeable rocks that result in low pressure gradient. On the other hand, in the regime of  $A > 0$ , these advancing distributions deform their shapes considerably due to phase transition whose front moves or stays independent of advection. In this case, the CIP scheme is not applicable because the scheme's accurate simulations of the advancing distributions maintaining their shape become misdirected efforts that degrade the reliability of numerical solutions and often result in numerical failures. Considering these regimes defined by the applicability index, we select the scheme to solve the advection terms from the CIP and first-order upstream difference schemes. Note that this evaluation of the applicability of the CIP scheme can be extended to other schemes of high-order accuracy, such as the TVD schemes adopted by Oldenburg and Pruess (2000) and Eulerian-Lagrangian schemes adopted by Croucher et al. (2004).

### 3.3 Modifying time step lengths

Time step length is modified dynamically to speed up the execution time and recovery when the Newton-Raphson iteration does not converge within the allowed number of iteration (50). If the iteration does not converge within the allowed number, then the iteration is restarted using the time step length multiplied by 0.5. On the other hand, if the iteration converges within the allowed number, then the time step length is multiplied by 1.01 for every step unless an output time or the ending time of the run is exceeded. For output and ending runs at times given arbitrarily, the time step length is matched to these times if the present time step length exceeds an output time or ending time. Even if this matched time step length becomes very short, it is not recovered to moderate length at the step after output for simplicity of the numerical code. This recovery procedure may be needed in practical simulations. The threshold of the convergence is  $10^{-3}$  of relative change in the unknowns at each grid point during a single iterative procedure. The threshold found by trial and error may seem to be coarse. The author infers that smaller thresholds than this value are not allowed because of the limitation of accuracy in approximating the Jacobian using finite differences.

**Table 1: Properties of the numerical solutions.**

	Run 1	Run 2
Initial conditions		
Pressure, MPa	0.1	3.0
Specific enthalpy, kJ/kg	335	1200
Boundary conditions	Constant at the initial value	
Source		
Flow rate, kg/s/m <sup>2</sup>	$1.0 \times 10^{-5}$	$3.0 \times 10^{-5}$
Specific enthalpy, kJ/kg	1000	700
Physical properties of rocks		
Permeability, m <sup>2</sup>	$1 \times 10^{-15}$	$1 \times 10^{-12}$
Porosity	0.1	0.9
Thermal conductivity, W/m/K	1.0	1.0
Density, kg/m <sup>3</sup>	2500	2500
Specific heat capacity, J/kg/K	800	800
Relative permeability		
Model type	Corey	Corey
Residual liquid saturation	0.3	0.3
Residual steam saturation	0.0	0.0
Applicable condition of the CIP scheme	$A < 10^{-3}$	$A < 10^{-3}$

## 4. NUMERICAL SOLUTIONS

### 4.1 Numerical code and its validation

The author developed the numerical code using the coding language Fortran supported by the compiler GFortran version 4.8.5 and validated it using two references. The first reference is the reservoir simulator HYDROTHERM, whose numerical solution was compared with that of this study adopting the first-order upstream difference scheme regardless of the applicability of the CIP scheme. The upstream weighting scheme for computing mass and enthalpy fluxes at block boundaries adopted in HYDROTHERM is mathematically equivalent to the first-order upstream difference scheme, so that the author verified whether the numerical solution of this study could reproduce that of HYDROTHERM. The second reference is the analytic solution of the advection equation. The author verified the reliability by comparing the output of the subroutine that solves advection terms adopting the CIP scheme with the analytic solution. The third-order accuracy with respect to time and space of the CIP scheme was verified by evaluating numerical error with various time step lengths and grid sizes.

## 4.2 Examples of numerical solutions

Two contrasting examples demonstrate the applicability of the CIP scheme. Let us consider an outflow from a source at  $x=800$  [m] between boundaries at  $x=0$  [m] and  $x=2000$  [m] that have constant values of pressure and specific enthalpy throughout runs. In the first example (Run 1), hot fluid with a specific enthalpy of 1000 kJ/kg is injected continuously at a rate of  $1.0 \times 10^{-5}$  kg/s/m<sup>2</sup> into an initially single-phase reservoir of uniform pressure 0.1 MPa and specific enthalpy 335 kJ/kg. A two-phase region expands successively from the source to the downstream region. The second example (Run 2) considers injecting cold fluid of a specific enthalpy of 700 kJ/kg at a rate of  $3.0 \times 10^{-5}$  kg/s/m<sup>2</sup> continuously into an initially two-phase reservoir of uniform pressure 3.0 MPa and specific enthalpy 1200 kJ/kg. In this case, a single-phase cold region expands from the source sweeping the initially two-phase region successively. The remarkable difference between two runs is pressure gradient throughout the runs because the permeability of Run 2 ( $1.0 \times 10^{-12}$  m<sup>2</sup>) is larger than that of Run 1 ( $1.0 \times 10^{-15}$  m<sup>2</sup>) by three orders of magnitude. In addition, Run 2 is given a very large porosity value of 0.9, whereas Run 1 is given 0.1. This results in higher temperature contrast at the cooling front with little heat exchange between the fluid and rock matrix in Run 2. The properties of Runs 1 and 2 are summarized in Table 1.

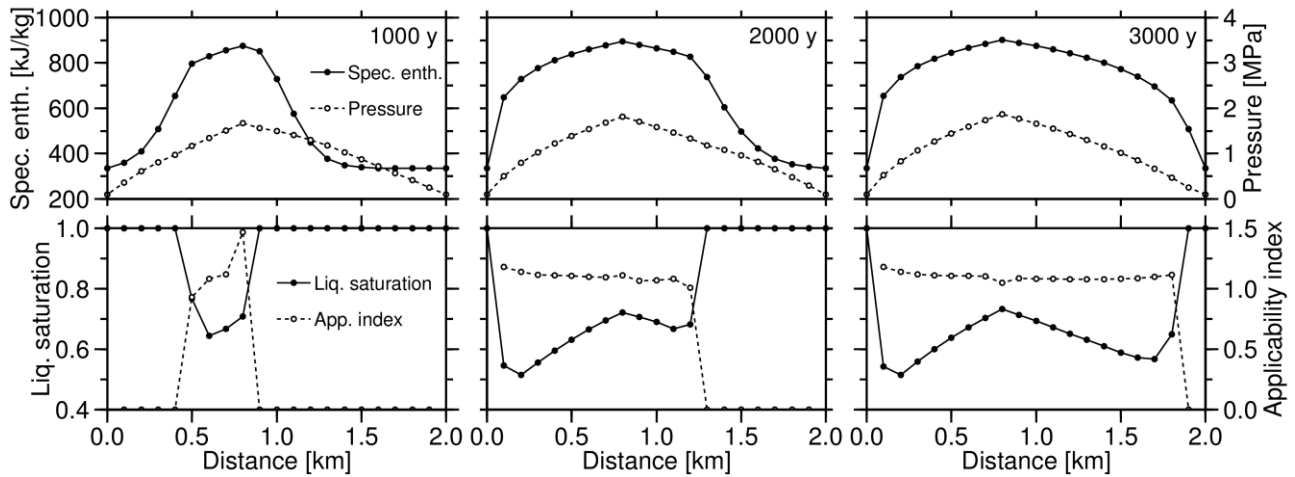


Figure 2: Numerical solution of Run 1.

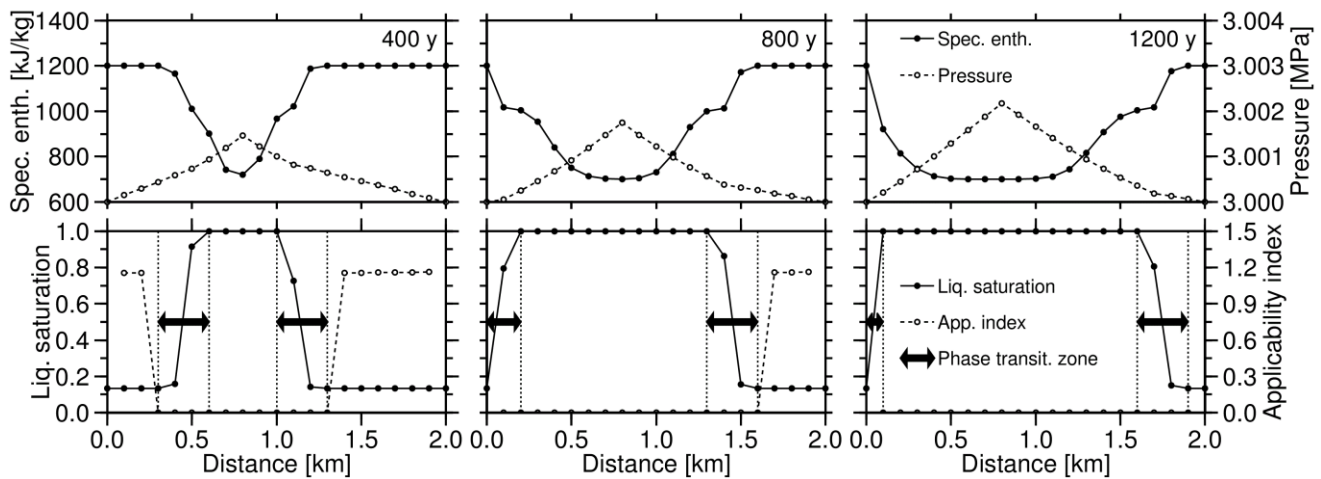


Figure 3: Numerical solution of Run 2.

The numerical solution of Run 1 is shown in Figure 2. The two-phase region expands from the source with advancing time and finally covers almost the entire domain of the numerical simulation at 3000 y. Liquid saturation remarkably increases with both increasing pressure and specific enthalpy. This feature indicates that the change in liquid saturation in the two-phase region is governed by pressure change predominantly and has little dependency on the change in specific enthalpy. The advancing distribution of specific enthalpy obeying advection has little control of the distribution of liquid saturation in the two-phase region. The applicability index in the two-phase region has a commonly higher value of near unity so that the CIP scheme is never applicable in the two-phase region in Run 1.

The numerical solution of Run 2 is shown in Figure 3. The single-phase region expands from the source sweeping the two-phase region with advancing time. In this case, the change in liquid saturation is strongly under control of the advancing distribution of specific

enthalpy because of the very small pressure gradients. As indicated by the applicability index, the CIP scheme is applicable in the single-phase region and the two-phase region of the phase transition zone where liquid saturation is changing from the initial value to unity. The higher value of the applicability index in the two-phase region out of the phase transition zone is caused by the initially uniform distribution of specific enthalpy. This initial uniform distribution never causes numerical dispersion in adopting any schemes, so that the inapplicability of the CIP scheme results in no obstacle practically.

### 4.3 Overcoming numerical failures

Figure 4 shows how the numerical failures were overcome in Run 1 by selecting the scheme for solving advection terms from the CIP and first-order upstream difference schemes based on the applicability index. The trial run that only adopted the CIP scheme regardless of the applicability index under the same conditions as Run 1 required nearly 12000 time steps, whereas Run 1 required nearly 5000 time steps (Figure 4a). This indicated that the Newton-Raphson iteration of the trial run did not converge frequently within the allowed number of iteration (50). In addition to this degradation of convergence, the oscillating distribution of liquid saturation was often observed in the trial run (Figure 4c). In another trial run that only adopted the CIP scheme regardless of the applicability index under the same conditions as Run 2, the author could not obtain the numerical solution for 1200 y as in Run 2. After advancing to over 100 y, the Newton-Raphson iteration was only able to converge with unrealistically short time step lengths of minus a few tenth power of ten years after repeated modification as described in Section 3.3. The author stopped the run after computing 50000 time steps.

The author infers that the abovementioned degradation of convergence and oscillating distribution of liquid saturation are caused by the misdirected approach in simulating the advection of mass and enthalpy for each phase that adopts the CIP scheme without considering the advancing phase transition front discussed in Section 3.2. The high accuracy of the CIP scheme in simulating pure advection with little numerical dispersion results in the unrecoverable inconsistency of this neglect. The overcoming of numerical failures by applying the first-order upstream difference scheme in the regime of large applicability indexes similar to Runs 1 and 2 is caused by intensive numerical dispersion generated by this scheme that obscures this inconsistency. Improving the numerical scheme by fully adopting the CIP scheme may involve the quantitative estimation of interaction between advection and advancing phase transition front.

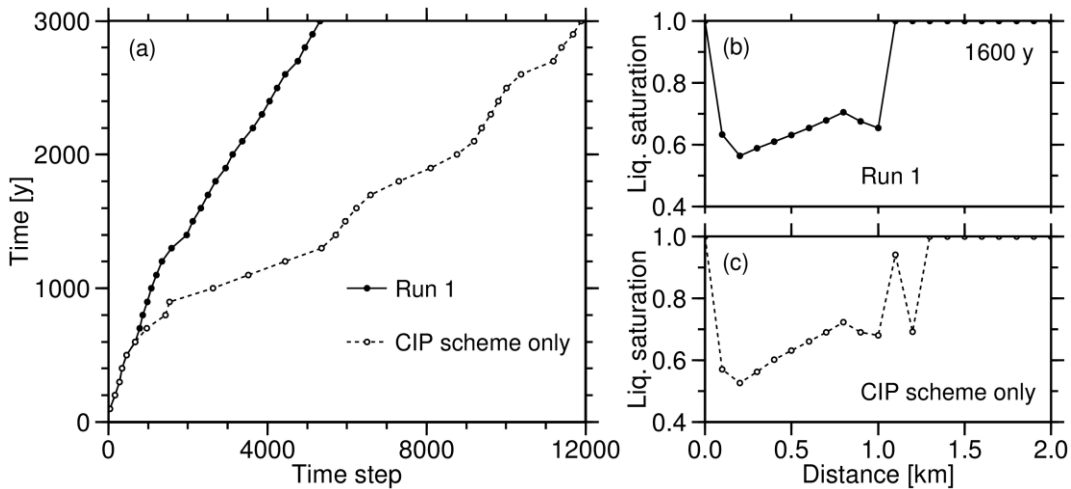


**Figure 4: Comparison between the numerical solutions of Run 1 and the trial run adopting the CIP scheme only regardless of the applicability index. (a) Advance of time with increasing time step. (b), (c) The distribution of liquid saturation at 1600 y simulated in each run.**

## 5. CONCLUSION

The applicability index indicating the valid condition of applying the CIP scheme has been defined. This index is derived schematically from the relative difference between the advancing velocities of the distribution of specific enthalpy due to flow and phase transition front. The application of the CIP scheme is only valid if the applicability index is strictly or nearly zero, which indicates that the phase transition is predominantly controlled by advection. The demonstrated numerical solutions have verified the effectiveness of selecting the scheme for solving advection terms from the CIP and first-order upstream difference schemes based on the applicability index. Adopting this hybrid scheme, the numerical failures, such as the degradation of convergence in the Newton-Raphson iteration and the oscillating distribution of liquid saturation, have been overcome successfully.

## NOMENCLATURE

### Latten symbols

- $A$  Applicability index.
- $c$  Specific heat capacity in J/kg/K.
- $H_g$  Enthalpy of gas phase per unit volume of rocks in J/m<sup>3</sup>,  $H_g = \phi \rho_g (1-S) h_g$ .

$H_l$	Enthalpy of liquid phase per unit volume of rocks in $J/m^3$ , $H_l = \phi \rho_l S h_l$ .
$H_m$	Enthalpy of matrix per unit volume of rocks in $J/m^3$ , $H_m = (1 - \phi) \rho_m c_m T$ .
$h$	Mean specific enthalpy of liquid and gas phases in $J/kg$ , $\{\rho_l S h_l + \rho_g (1 - S) h_g\} / \{\rho_l S + \rho_g (1 - S)\}$ .
$h_g, h_l$	Specific enthalpy of gas and liquid phase, respectively in $J/kg$ .
$h'$	Specific enthalpy of saturated water in $J/kg$ .
$k$	Permeability in $m^2$ .
$k_r$	Relative permeability.
$M_g$	Mass of gas phase per unit volume of rocks in $kg/m^3$ , $M_g = \phi \rho_g (1 - S)$ .
$M_l$	Mass of liquid phase per unit volume of rocks in $kg/m^3$ , $M_l = \phi \rho_l S$ .
$P$	Pressure in Pa.
$q_H$	Source flow rate of enthalpy in $W/m^3$ .
$q_M$	Source flow rate of mass in $kg/s/m^3$ .
$S$	Liquid saturation.
$T$	Temperature in $^{\circ}C$ .
$t$	Time in s.
$U_g$	Flow velocity of gas phase in m/s, $U_g = -k_{rg} k / \{\phi (1 - S) \mu_g\} \cdot \partial_x P$ .
$U_l$	Flow velocity of liquid phase in m/s, $U_l = -k_{rl} k / \{\phi S \mu_l\} \cdot \partial_x P$ .
$u$	Advancing velocity of the distribution of specific enthalpy due to flow.
$u'$	Advancing velocity of the phase transition front.
$x$	Coordinate in m.

### Greek symbols

$\theta_M, \theta_H$	Non-advection terms of mass and enthalpy conservation equations (Eq. (1) and (2)), respectively.
$\lambda$	Thermal conductivity of rocks in $W/m/K$ .
$\mu_g, \mu_l$	Viscosity of gas and liquid phase, respectively, in Pa s.
$\rho_g, \rho_l$	Density of gas and liquid phase, respectively, in $kg/m^3$ .
$\Phi$	Arbitrary variable.
$\phi$	Porosity.

### Subscripts

$g$	Gas phase.
$l$	Liquid phase.
$m$	Rock matrix.
$p$	Arbitrary phase.
$x$	Partial derivative with respect to $x$ .

### REFERENCES

- Anderson, E., Bai, Z., Bischof, C., Blackford, S., Demmel, J., Dongarra, J., Du Croz, J., Greenbaum, A., Hammarling, S., Mckenney, A., and Sorensen, D.: LAPACK Users' Guide Third Edition, Society for Industrial and Applied Mathematics, (1999), 429 pp.
- Croucher, A.E., O'Sullivan, M.J., Kikuchi, T., and Yasuda, Y.: Eulerian-Lagrangian tracer simulation with TOUGH2, *Geothermics*, **33**, (2004), 503-520.
- IAPWS: Revised Release on the IAPS Formulation 1985 for the Viscosity of Ordinary Water Substance, The International Association for the Properties of Water and Steam (IAPWS), (1997), 15 pp.
- IAPWS: Supplementary Release on Backward Equations for Pressure as a Function of Enthalpy and Entropy  $p(h,s)$  to the IAPWS Industrial Formulation 1997 for the Thermodynamic Properties of Water and Steam, The International Association for the Properties of Water and Steam (IAPWS), (2001), 13 pp.
- IAPWS: Revised Supplementary Release on Backward Equations for the Functions  $T(p,h)$ ,  $v(p,h)$  and  $T(p,s)$ ,  $v(p,s)$  for Region 3 of the IAPWS Industrial Formulation 1997 for the Thermodynamic Properties of Water and Steam, The International Association for the Properties of Water and Steam (IAPWS), (2004a), 22 pp.
- IAPWS: Supplementary Release on Backward Equations  $p(h,s)$  for Region 3, Equations as a Function of  $h$  and  $s$  for the Region Boundaries, and an Equation  $T_{sat}(h,s)$  for Region 4 of the IAPWS Industrial Formulation 1997 for the Thermodynamic Properties of Water and Steam, The International Association for the Properties of Water and Steam (IAPWS), (2004b), 34 pp.

Matsumoto

- IAPWS: Supplementary Release on Backward Equations for Specific Volume as a Function of Pressure and Temperature  $v(p,T)$  for Region 3 of the IAPWS Industrial Formulation 1997 for the Thermodynamic Properties of Water and Steam, The International Association for the Properties of Water and Steam (IAPWS), (2005), 35 pp.
- IAPWS: Revised Release on the IAPWS Industrial Formulation 1997 for the Thermodynamic Properties of Water and Steam, The International Association for the Properties of Water and Steam (IAPWS), (2007), 49 pp.
- Kipp Jr., K.L., Hsieh, P.A., and Charlton, S.R.: Guide to the Revised Ground-Water Flow and Heat Transport Simulator: HYDROTHERM-Version 3, *U.S. Geological Survey Techniques and Methods*, **6-A25**, (2008), 160 pp.
- Matsumoto, M.: Improving the Numerical Accuracy of Hydrothermal Reservoir Simulations Using the CIP Scheme with Third-Order Accuracy, *Proceedings, 37th Workshop on Geothermal Reservoir Engineering*, Stanford University, Stanford, CA (2012).
- Matsumoto, M.: Application of the Constrained Interpolation Profile (CIP) Scheme to Two-Dimensional Single-Phase Hydrothermal Reservoir Simulations, *Geothermics*, **54**, (2015), 10-22.
- Oldenburg, C.M. and Pruess, K.: Simulation of propagating fronts in geothermal reservoirs with the implicit Leonard total variation diminishing scheme, *Geothermics*, **29**, (2000), 1-25.
- Yabe, T. and Aoki, T.: A Universal Solver for Hyperbolic Equations by Cubic-Polynomial Interpolation I. One-Dimensional Solver, *Comput. Phys. Commun.*, **66**, (1991), 219-232.
- Yabe, T., Ishikawa, T., Wang, P.Y., Aoki, T., Kadota, Y., and Ikeda, F.: A Universal Solver for Hyperbolic Equations by Cubic-Polynomial Interpolation II. Two- and Three-Dimensional Solvers, *Comput. Phys. Commun.*, **66**, (1991), 233-242.